



Contents lists available at ScienceDirect

Bioorganic & Medicinal Chemistry Letters

journal homepage: www.elsevier.com/locate/bmcl

Synthesis and biological evaluation of 9-fluorenone derivatives for SPECT imaging of $\alpha 7$ -nicotinic acetylcholine receptor

Hang Gao, Shuxia Wang, Yueheng Qi, Guoxue He, Bingchao Qiang, Sixuan Wang, Huabei Zhang*

Key Laboratory of Radiopharmaceuticals of Ministry of Education, College of Chemistry, Beijing Normal University, No. 19 Xinjiekouwai Street, Haidian District, Beijing 100875, China

ARTICLE INFO

Keywords:

$\alpha 7$ -Nicotinic acetylcholine receptors ($\alpha 7$ -nAChRs)
SPECT/CT
Radiotracers
Alzheimer's disease

ABSTRACT

The $\alpha 7$ -nicotinic acetylcholine receptor ($\alpha 7$ -nAChR) subtype, is found to have a connection with the pathogenesis of a variety of psychiatric and neurological disorders. Herein, we report the development of radioiodinated 9-fluorenone derivatives as single-photon emission computed tomography (SPECT) imaging tracers for $\alpha 7$ -nAChRs. Among the derivatives, the best member of the series **10** ($K_i = 2.23$ nM) were radiolabeled with ^{125}I for *in vitro* and *in vivo* studies. The radiotracer [^{125}I]**10** exhibited robust brain uptake and specifically labeled $\alpha 7$ -nAChRs with a peak uptake value of $9.49 \pm 0.87\%$ ID/g in brain. Blocking studies demonstrated that the tracer was highly specific toward $\alpha 7$ -nAChR. Furthermore, *ex vivo* autoradiography and micro-SPECT/CT dynamic imaging in mice confirmed the excellent imaging properties. In addition, molecular docking was also performed to rationalize the potency of the chosen compounds towards $\alpha 7$ -nAChRs. To conclude, compound **10** could serve as a promising radiotracer for the $\alpha 7$ -nAChRs.

Introduction

The neurotransmitter acetylcholine (ACh) exerts its work on the cardiovascular, immune system and the central and peripheral nervous systems. Acetylcholine receptors (AChRs) which comprised different multimers, are divided into a neuronal type ($\alpha 2$ - $\alpha 10$ and $\beta 2$ - $\beta 4$) and a muscle type ($\alpha 1$, $\beta 1$, γ , δ and ϵ). Different subunits may assembled into numerous receptor subtypes.¹ Among subtypes, nicotinic acetylcholine receptors (nAChRs) which belong to the superfamily of ligand-gated ion channels, are composed of five transmembrane proteins in a pentameric structure.² In human brain, $\alpha 7$ -nAChRs and $\alpha 4\beta 2$ subtypes are predominant.³

Research from biological studies revealed that the $\alpha 4\beta 2$ -nAChR subtype in the central nervous system (CNS) has a high binding affinity to nicotine, while homomeric $\alpha 7$ -nAChRs possess strong binding to methyllycaconitine (MLA) or α -bungarotoxin (α -Bgt) and have a high permeability to calcium.⁴ While nAChRs coordinate synaptic delivery at muscle end-plates or functioning autonomic ganglia in the peripheral nervous system, different subtypes of nicotinic acetylcholine receptors in the CNS play their respective roles on regulating physiology, such as sensorimotor gating, memory, metabolism and inflammation. The $\alpha 7$ -nAChR subtype, is found to have a connection with the pathogenesis of a variety of psychiatric and neurological disorders, including Alzheimer's disease (AD), schizophrenia (SCZ), anxiety, depressive disorder,

inflammation and substance dependence.⁵

Due to the distribution and quantity of $\alpha 7$ -nAChRs in the CNS, this receptor type has become a potential therapeutic target for mental disorders. Clinical experiments of $\alpha 7$ -nAChR agonists revealed that $\alpha 7$ -nAChRs partial agonists can help improve cognitive performance in people with SCZ.⁶ Meanwhile, numerous postmortem studies have shown a reduction of $\alpha 7$ -nAChRs in the cerebral tissues of SCZ patients, with similar findings appearing in AD patients.⁷ Although numerous studies have tried to elucidate the mechanisms of $\alpha 7$ -nAChRs, in the brain these mechanisms are not fully understood. Nevertheless, a small numbers of therapies aimed at $\alpha 7$ -nAChRs has been applied to clinical trials.⁸ However, invalid cases of the planned therapies occurred in clinical trials, emphasized a strong demand for a biomarker to monitoring the pathological processes in preclinical research. Therefore, it is undoubtedly crucial to develop a human compatible $\alpha 7$ -nAChR radiotracer for early diagnosis and to evaluate the efficiency of drug therapies in clinical trials for the treatment of SCZ or AD.

In vivo imaging and quantifying $\alpha 7$ -nAChRs in the human brain provide a solution to develop such a biomarker. Positron-emission tomography (PET) and single-photon emission computed tomography (SPECT) offer an advanced and suitable way to quantify cerebral receptors and their occupancy *in vivo*.

Numerous $\alpha 7$ -nAChR ligands have been labeled with ^{11}C , ^{18}F or ^{125}I ,⁹ such as [^{125}I]**1**,¹⁰ [^{125}I]Iodo-ASEM,¹¹ [^{11}C]CHIBA-1001,¹² [^{18}F]

* Corresponding author.

E-mail addresses: hgao@mail.bnu.edu.cn (H. Gao), hbzhang@bnu.edu.cn (H. Zhang).

<https://doi.org/10.1016/j.bmcl.2019.126724>

Received 2 August 2019; Received in revised form 22 September 2019; Accepted 28 September 2019

0960-894X/© 2019 Elsevier Ltd. All rights reserved.

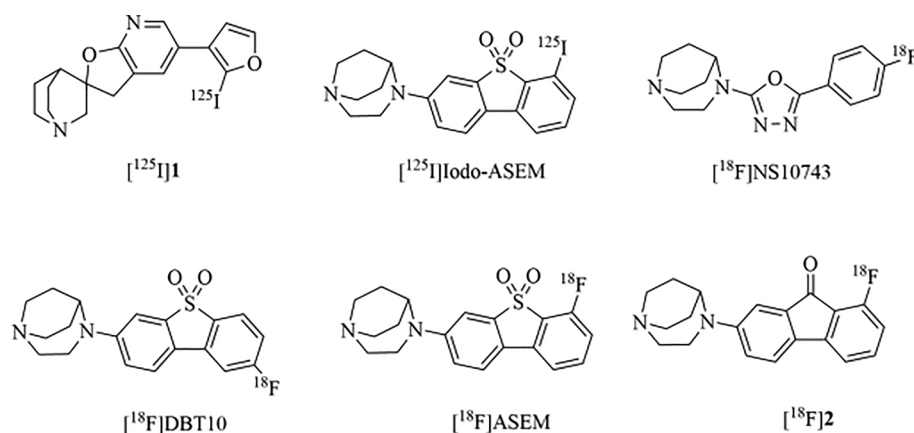


Fig. 1. Representative $\alpha 7$ -nAChRs radioligands.

NS10743,¹³ [¹⁸F]ASEM,¹⁴ [¹⁸F]DBT10 and [¹⁸F]2 (Fig. 1).^{15,16} Despite some of them showing low brain uptake or binding specificity, two promising ¹⁸F labeled $\alpha 7$ -nAChR ligands [¹⁸F]DBT10 ($K_i = 1.3$ nM) and [¹⁸F]ASEM ($K_i = 0.4$ nM) have been tracked in primates and non-primates studies.^{15,17} Together with [¹⁸F]2 ($K_i = 2.98$ nM), these three compounds are the most promising agents for human $\alpha 7$ -nAChR PET imaging. We envisioned the synthesis of iodo derivatives of 2 would producing a new set of compounds with similar potency and the potential for radiolabeling with ¹²³I and ¹²⁵I for SPECT imaging.

Here we report [¹²⁵I]Iodo-10, the radio-iodinated analog of fluorenone-9-one designed for usage in cell-based assays of $\alpha 7$ -nAChRs and as potential probes for SPECT imaging *in vivo* studies. The studied ligand is amenable to labeling with ¹²³I and serve as human $\alpha 7$ -nAChR radiotracers for SPECT studies. In addition, molecular docking confirmed the binding modes of the promising ligand.

Results and discussions

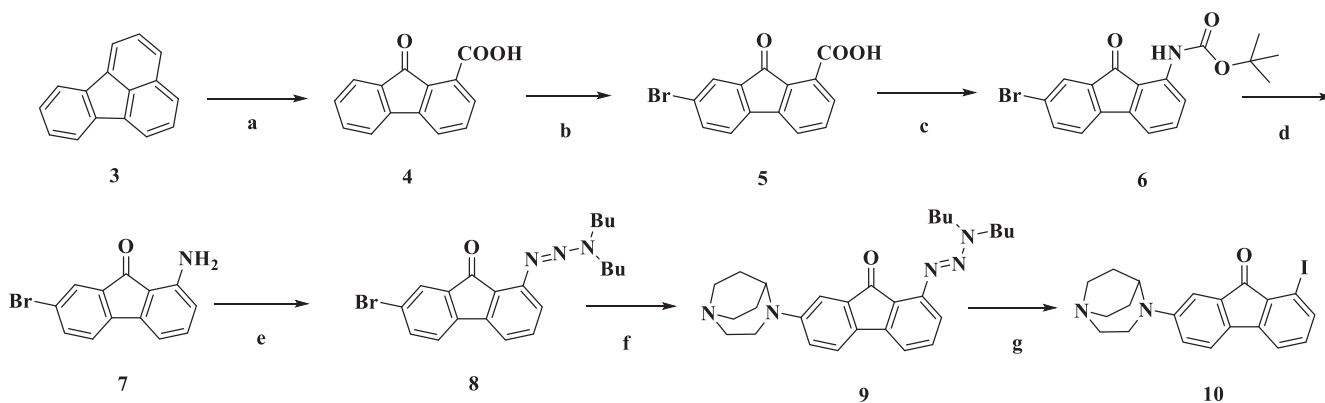
The synthetic routes for the ortho-iodine substitution compounds 10 are shown in Scheme 1. Fluoranthene (3) was oxidized to open the loop by chromium (VI) oxide and efficiently brominated to carboxylic acid 5. After Curtius rearrangement by a one pot reaction, a Boc-protected aniline 6 was generated by replacing the carboxy group of 5. The Boc-protecting group of 6 was removed by 1 N HCl and then diazotized using sodium nitrite in hydrochloric acid solution. After the diazo coupled with dibutylamine, a triazene compound 8 was generated. The precursor 9 was synthesized by Buchwald-Hartwig cross-coupling reaction between 1,4-diazabicyclo[3.2.2]nonane and compound 8. The nonlabelled standard 10 was obtained by TFA pretreating 9 in a sodium

iodide aqueous solution.

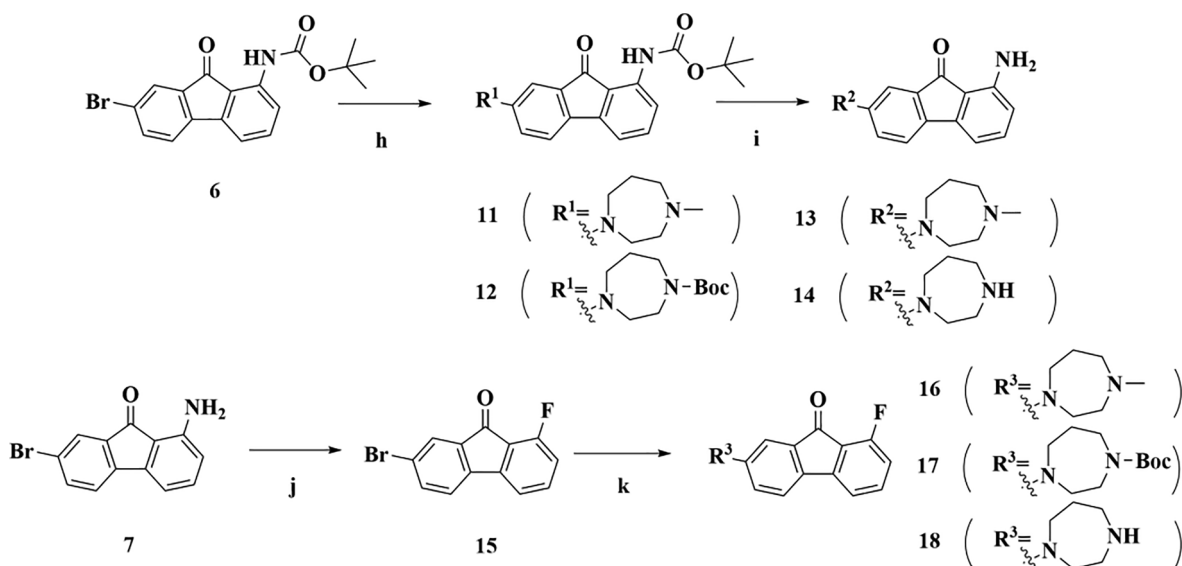
The synthesis routes of the 1,4-diazepan-1-yl substitution compounds 11–17 are outline in Scheme 2. The compounds 11 and 12 were prepared by Buchwald-Hartwig cross-coupling reaction with heterocyclic ring and Boc-protected aniline 6. The final amino substituted 13 and 14 were further obtained by removal of the Boc-protecting group. The fluorine substitutes compound 15 was obtained via the Schiemann reaction, and the final fluorine substitutes compound 16, 17 and 18 were synthesized using the similar steps as 11, 12 and 14.

To measure the *in vitro* binding affinity and selectivity of the synthesized $\alpha 7$ -nAChRs ligands and precursors, *in vitro* competition binding assays of $\alpha 7$ -nAChRs and $\alpha 4\beta 2$ subtypes were performed. Both of the $\alpha 7$ and $\alpha 4\beta 2$ -nAChR assays were performed using rat cortical membranes. The binding assays of $\alpha 7$ -nAChRs were tested *in vitro* competition with 0.4 nM [¹²⁵I] α -bungarotoxin ([¹²⁵I] α -Bgt), which is an $\alpha 7$ -nAChR antagonist ($K_D = 0.7$ nM). Furthermore, MLA, a specific $\alpha 7$ -nAChR antagonist was tested as the reference compound to ensure the reliability and comparison of the method (Table 1).

Among the new series of compounds, 10 showed the highest binding affinity for pentamer- $\alpha 7$ -nAChRs with K_i values of 2.23 nM and is almost equally matched to that previously reported [¹⁸F]2 ($K_i = 2.98$ nM) and are the same level as ASEM ($K_i = 0.37$ nM) and iodo-ASEM ($K_i = 0.93$ nM).^{14,16} 10 exhibited much the same as the reference $\alpha 7$ -nAChRs ligand MLA, whereas the binding affinity of heterocycle substitutes compounds were lower. The potential precursors 9 was studied under the same conditions but showed poor results. The 1,4-diazepan-1-yl and the 4-methyl-1,4-diazepan-1-yl substitutes showed moderate binding affinities in the range of 70 to 100 nM. The amino-substituted fluorenone exhibited a slight higher potency than



Scheme 1. Synthesis of iodinated ortho-substitution compound 10. Reagents and conditions: (a) CrO₃, H₂O, CH₃COOH, 80–85 °C, 110–120 °C; (b) Br₂, 80–85 °C; (c) Et₃N, DPPA, *t*-BuOH, toluene, 110 °C; (d) CH₃CN, 1 N HCl, 80 °C, 1 N NaOH; (e) NaNO₂, CH₃CN, HCl, dibutylamine, K₂CO₃, –5 °C, RT; (f) Cs₂CO₃, Pd₂(dba)₃, BINAP, toluene, 85 °C; (g) TFA, NaI, MeCN, H₂O, 80 °C.



Scheme 2. Synthesis of **11–17**. Reagents and conditions: (h) Cs_2CO_3 , $\text{Pd}_2(\text{dba})_3$, BINAP, toluene, 85°C ; (i) CH_3CN , 1 N HCl, 80°C , 1 N NaOH; (j) Et_3N , DPPA, *t*-BuOH, toluene, 110°C ; (k) HBF_4 , $0\text{--}5^\circ\text{C}$; NaNO_2 ; H_2O , 120°C ; (k) Cs_2CO_3 , $\text{Pd}_2(\text{dba})_3$, BINAP, toluene, 80°C .

Table 1

In vitro binding affinities (K_i , nM) of MLA, nicotine, and the new series **9**, **10**, **13**, **14**, **15** for $\alpha 7$ -nAChR and $\alpha 4\beta 2$ subtypes.

Compd	K_i (nM)		Selectivity $\alpha 7/\alpha 4\beta 2$
	$\alpha 7^a$	$\alpha 4\beta 2^b$	
MLA	2.68 ± 0.85	nt ^c	
Nicotine	nt ^c	3.8 ± 1.15	
10	2.23 ± 0.56	6517 ± 658	2922
13	77.9 ± 4.45	9842 ± 357	126
14	88.1 ± 9.21	$> 10 \mu\text{M}$	
16	80.1 ± 5.21	9631 ± 514	120
18	92.5 ± 4.11	$> 10 \mu\text{M}$	

^a SD rat (female, 180–270 g) cerebral cortex; radiotracer, [^{125}I] α -Bgt (0.4 nM), $K_D = 0.7$ nM; K_i values are the means \pm SD of assays performed in triplicate.

^b SD rat (female, 180–270 g) cerebral cortex; radiotracer, [^3H]cytisine (1 nM), $K_D = 0.77$ nM; K_i values are the means \pm SD of assays performed in triplicate.

^c nt: not tested.

fluorine-substituted compounds, indicating an interaction with $\alpha 7$ -nAChRs may exist. For the heterocycle substitutes groups on the other sides, a loss of potency occurred when changing the 1,4-diazabicyclo [3.2.2]nonane to the diazepam substitutes.

Heteromeric $\alpha 4\beta 2$ -nAChR is the main nicotinic acetylcholine receptor subtype, so we also performed the binding assays using [^3H]cytisine (1 nM) as the competing radioligand (Table 1). The $\alpha 4\beta 2$ subtype affinities of the tested compounds were obviously larger than the corresponding $\alpha 7$ -nAChR affinities which indicate good $\alpha 7$ -nAChR/ $\alpha 4\beta 2$ -nAChR selectivity. **10** showed excellent selectivity where the diazepam substitutes **13** and **16** manifested lower selectivity.

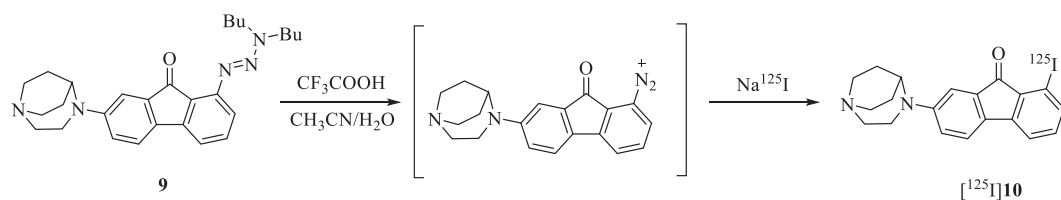
We radiolabeled the **10** as shown in Scheme 3. [^{125}I]**10** was prepared by the reaction of precursor **9** acidized by TFA and Na^{125}I (Na^{125}I

in 0.1 N NaOH) in a mixed solution of acetonitrile and water as the solvent. The obtained crude was purified by high-performance liquid chromatography (HPLC) followed by extraction on an SPE cartridge. The final product of [^{125}I]**10** was eluted at 41.61 min and obtained with a radiochemical yield of 31.8% and a high radiochemical purity ($> 98\%$). The specific activity of [^{125}I]**10** was 62.9 GBq/mmol (1700 Ci/mmol). [^{125}I]**10** was authenticated by comparing its retention time with its standard substance **10** via coinjection in HPLC. The retention times of [^{125}I]**10** and **10** were 7.26 min and 6.93 min respectively which matched were within admissible error levels (Fig. 2).

To confirmed the stability of studied radiotracer, the *in vitro* stability of [^{125}I]**10** in fetal bovine serum at 37°C , and in saline at room temperature was determined by assessing radiochemical purity via HPLC after incubating respectively. The radiochemistry purities of the studied compounds in serum and saline were all $> 98\%$ after 12 h (Fig. 3), which demonstrated the high *in vitro* biostability of radioligands [^{125}I]**10**.

For the biodistribution studies of [^{125}I]**10**, it showed a high brain uptake after intravenous injection (0.2 μCi , in 0.1 mL saline, containing 10% ethanol). [^{125}I]**10** exhibited a robust brain uptake of 6.47 ± 0.41 %ID/g at 5 min postinjection, then quickly reached the peak uptake value of 9.49 ± 0.87 %ID/g in the brain at 15 min (Table 2). The brain15min/brain120min value was 2.91 which was a reasonable clearance rate for brain SPECT imaging. Among the remaining organs, the thyroid uptake, which was crucial for ^{125}I -radiolabeled ligands, showed relatively low values within an hour. The highest uptake of [^{125}I]**10** in the thyroid was 3.61 ± 0.21 %ID at 120 min, indicating a good stability of the iodide group *in vivo*. The blood uptake was fairly low, a high brain/blood ratio of 8.11 at 15 min postinjection was measured. Lung uptake displayed an idiosyncratic value of 50.78 ± 8.72 %ID/g at 5 min, but a fast clearance.

To better illustrate the distribution of the radiotracer in brain, [^{125}I]



Scheme 3. Radiosynthesis of [^{125}I]**10**.

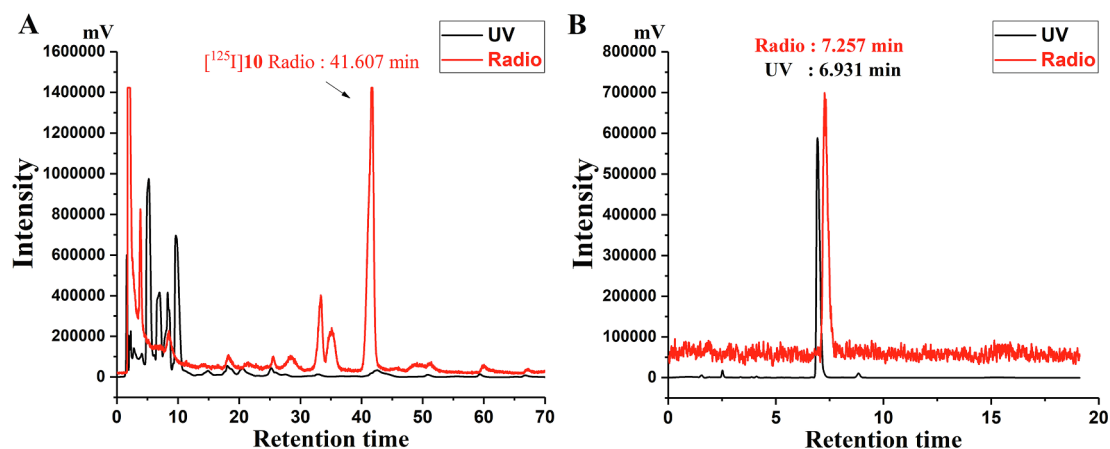


Fig. 2. (A) HPLC chromatogram of preparation of $[^{125}\text{I}]\mathbf{10}$. (B) Coinjection of $[^{125}\text{I}]\mathbf{10}$ and $\mathbf{10}$.

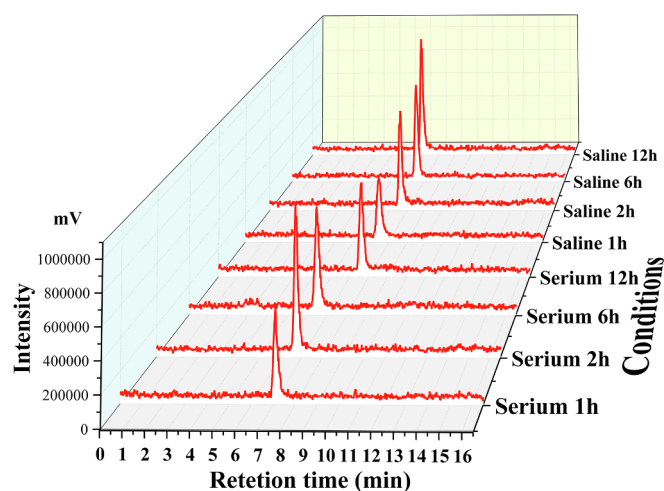


Fig. 3. HPLC chromatograms of $[^{125}\text{I}]\mathbf{10}$ in fetal bovine serum and saline, for 1–12 h.

$\mathbf{10}$ were tested in Kunming mice as potential SPECT tracers for imaging cerebral $\alpha 7$ -nAChRs (Fig. 4). After tail vein injection, $[^{125}\text{I}]\mathbf{10}$ exhibited rapid initial brain uptake and quickly reached peak uptake in the brain at 15 min, followed by a moderate washout. The peak concentration of radioactivity of iodine-radiotracer appeared in the frontal cortex, striatum and the superior and inferior colliculi. The uptake values of

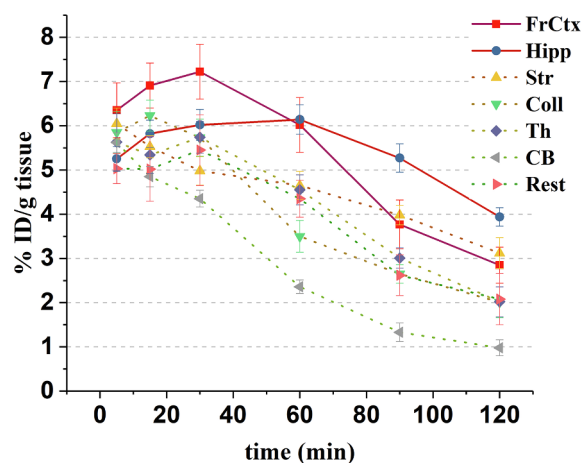


Fig. 4. Biodistribution of $[^{125}\text{I}]\mathbf{10}$ in the cerebral regions of mice. Data are expressed as the percentage of injected dose per gram (%ID/g), mean \pm SD, $n = 3$. Abbreviations: FrCtx, frontal cortex; Hipp, hippocampus; Str, striatum; Coll, superior and inferior colliculi; Th, thalamus; CB, cerebellum. Rest, rest of the brain.

$[^{125}\text{I}]\mathbf{10}$ at 30 min in frontal cortex, hippocampus or superior and inferior colliculi were 7.22 ± 0.62 %ID/g, 5.73 ± 0.42 %ID/g and 6.02 ± 0.35 %ID/g respectively. Moderate uptake of the ligand was observed in the striatum and thalamus; while the cerebellum had the lowest uptake. The distribution of radioiodo-labelled $[^{125}\text{I}]\mathbf{10}$ was in

Table 2
Biodistribution of $[^{125}\text{I}]\mathbf{10}$ in Kunming mice (female, 18–22 g).^a

Organs	Time (min)					
	5 min	15 min	30 min	60 min	120 min	
Blood	1.87 \pm 0.21	1.17 \pm 0.19	1.10 \pm 0.32	0.70 \pm 0.27	0.52 \pm 0.13	
Brain	6.47 \pm 0.41	9.49 \pm 0.87	8.03 \pm 0.73	6.21 \pm 0.32	3.26 \pm 0.15	
Thyroid ^b	0.22 \pm 0.09	0.65 \pm 0.12	0.93 \pm 0.14	1.51 \pm 0.24	3.61 \pm 0.21	
Heart	8.96 \pm 0.87	4.21 \pm 0.21	3.50 \pm 0.18	4.48 \pm 0.29	1.67 \pm 0.16	
Liver	7.62 \pm 0.65	13.56 \pm 0.86	16.35 \pm 0.41	9.61 \pm 0.56	5.84 \pm 0.57	
Spleen	4.62 \pm 0.32	8.07 \pm 0.63	10.19 \pm 0.97	6.30 \pm 0.51	4.03 \pm 0.44	
Lung	50.78 \pm 8.72	29.52 \pm 2.84	24.85 \pm 1.45	11.20 \pm 0.97	5.17 \pm 0.84	
Kidney	16.42 \pm 1.04	12.48 \pm 1.25	9.89 \pm 0.76	5.63 \pm 0.47	4.21 \pm 0.87	
Muscle	2.16 \pm 0.57	3.74 \pm 0.94	3.85 \pm 0.46	2.29 \pm 0.31	1.30 \pm 0.18	
Bone	1.03 \pm 0.35	1.31 \pm 0.39	2.71 \pm 0.20	2.37 \pm 0.51	2.83 \pm 0.23	
Intestine	1.42 \pm 0.15	1.84 \pm 0.17	6.43 \pm 0.39	5.51 \pm 0.55	2.83 \pm 0.21	
Stomach	1.57 \pm 0.40	1.83 \pm 0.21	6.76 \pm 1.02	5.32 \pm 0.80	3.26 \pm 0.47	
Brain/Blood	3.50	8.11	7.30	8.87	6.26	

^a Data are expressed as the percentage of injected dose per gram (%ID/g), mean \pm SD, $n = 3$.

^b Data are expressed as the percentage of injected dose (%ID), mean \pm SD, $n = 3$.

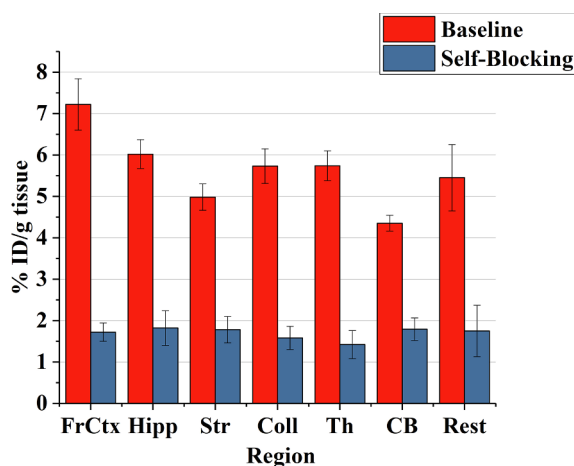


Fig. 5. Inhibition of [125 I]10 in mice brain regions. Data are mean \pm SD (n = 3). Abbreviations: FrCtx, frontal cortex; Hipp, hippocampus; Str, striatum; Coll, superior and inferior colliculi; Th, thalamus; CB, cerebellum. Rest, rest of the brain.

accordance with the biodistribution of $\alpha 7$ -nAChRs in rodents.¹⁹ The ratio of radiotracers uptake in the whole brain tissue to that in the cerebellum was 7.38 at 15 min and reached 12.3 after 60 min. The clearance rate of the studied tracer from the cerebellum was faster than from other regions. The ratios of [125 I]10 are highly consistent with the results of the *in vitro* $\alpha 7$ -nAChR binding assays.

Self-blockade studies of [125 I]10 with its nonlabeled standards were also conducted to ensure specificity (Fig. 5). The results showed an evident reduction of uptake among all regions of the brain, which demonstrated the specificity of the studied radiotracers. For [125 I]10, the cortex, superior and inferior colliculi and hippocampus had a blockade ratio of 76.2%, 69.8%

and 75.1% respectively. The results indicated that the [125 I]10 was specific to regions rich in $\alpha 7$ -nAChRs, except for the cerebellum which still had a moderate concentration. The deviation may due to the time point that brain tissues were harvested was corresponded to the peak concentration of brain uptake, which leads to uncontrolled factors.

To further determine the specificities of [125 I]10 to $\alpha 7$ -nAChRs over other nAChRs or similar subtypes, independent experiments of the blocking studies were carried out by intravenous preinjection of three blocking agents. We chose SSR180711, a selective $\alpha 7$ -nAChR partial agonist with good affinity, to study *in vivo* selectivity.²⁰ For the non- $\alpha 7$ -nAChR, $\alpha 4\beta 2$ -nAChR and 5-HT₃ receptors, we chose cytosine and ondansetron for the blocking agents.²¹ In this study, SSR180711, cytosine and ondansetron were preinjected 15 min before the injection of the radiotracers. Saline was preinjected either in the control group to avoid issues of interference. The mice were sacrificed at 100 min postinjection of the radiotracers, and brain tissues were harvested. The SSR180711 blocking group showed an obvious reduction of radioactivity, the inhibitor ratio was greater than 60% suggesting that [125 I]10 was specific to $\alpha 7$ -nAChRs (Fig. 6).

Meanwhile in the group of cytosine and ondansetron blocking, radioactivity accumulation in the frontal cortex, hippocampus and striatum for [125 I]10 was not reduced, with an inhibitor ratio less than 15% which indicated that [125 I]10 was selective for $\alpha 7$ -nAChRs versus $\alpha 4\beta 2$ subtypes and 5-HT₃ receptors. Moreover, three blocking agents had almost no effect on accumulation of radioactivity in the cerebellum, suggesting that [125 I]10 in the cerebellum had nonspecific binding.

The *ex vivo* autoradiography was performed and cross-referenced with mouse brain atlases to characterize [125 I]10 as possible imaging probes.²² As shown in Fig. 7, the radiotracer [125 I]10 exhibited intensive labeling, showing a strong signal in the frontal cortex, thalamus, hypothalamus, hippocampus and striatum, where $\alpha 7$ -nAChRs were

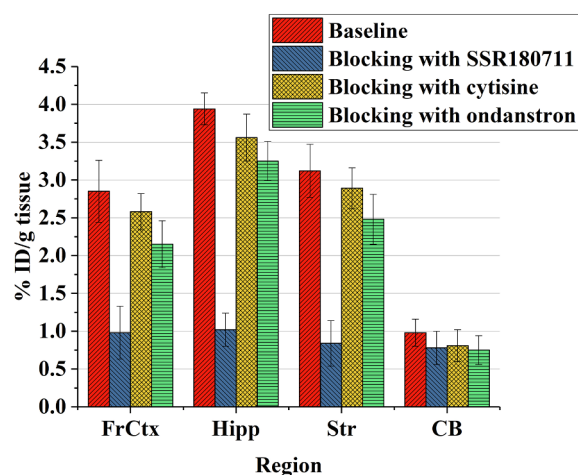


Fig. 6. Blocking studies of [125 I]10 with selective $\alpha 7$ -nAChR, $\alpha 4\beta 2$ -nAChR and 5-HT₃ ligands in Kunming mice. Data are mean \pm SD (n = 3). Blocking studies of [125 I]10 with intravenous preinjection of SSR180711 (1 mg/kg), cytosine (1 mg/kg) and ondansetron (2 mg/kg). Abbreviations: FrCtx, frontal cortex; Hipp, hippocampus; Str, striatum; CB, cerebellum.

highly expressed. To further determine whether the *in vivo* binding of [125 I]10 in the brain could be inhibited by selective agonist, SSR180711 was used as a blocker. As shown in Fig. 7B the ligand was significantly blocked in Kunming mice, which again confirmed its specificity and selectivity. [125 I]10 showed effective labeling of $\alpha 7$ -nAChRs and minimal background labeling proving that the tracer is a suitable radioprobe of $\alpha 7$ -nAChR for *in vivo* studies.

Dynamic SPECT/CT studies of [125 I]10 was successively obtained on Kunming mice (female, 18–22 g) after intravenous injection of radioiodinated probes (0.1 mL, 80 μ Ci, 2.96 MBq). Mice were anesthetized with isoflurane for imaging and conducted with the 60 min consecutive dynamics SPECT/CT study. Furthermore, two more static scanning (90 min, 120 min postinjection) were also performed to study the internal retention and metabolism of the radioligands in mice. As shown in Fig. 8A, significant and robust brain uptake was observed postinjection. In agreement with the biodistribution results discussed above, [125 I]10 reached maximum radioactive concentration at 15–20 min postinjection. Deiodination was hardly to be observed during the study in 60 min, which was in accordance with the *in vitro* stability study and further demonstrated its *in vivo* stability. [125 I]10 had a good retention and moderate washout in the mouse brain. The accumulation in brain was gradually decreased after 60 min and reached the same radioactive level with thyroid at 120 min. The imaging results are consistent with the experimental data performed above and further demonstrate that [125 I]10 could be a potential SPECT radiotracer for *in vivo* imaging of human $\alpha 7$ -nAChRs.

To further ensure the brain uptake or distribution of the radioactive substance in $\alpha 7$ -nAChR blocked Kunming mice, blocking studies of [125 I]10 compounds were conducted. As shown in Fig. 8B, following injection of SSR180711 (1 mg/kg) 15 min before radiotracer injection, a significant reduction of uptakes was observed at 30 min and 60 min postinjection. Therefore, the SPECT/CT blocking imaging study, in combination with the results of the dynamics studies and *in vivo/vitro* experiments discussed above, indicated that radioiodinated tracer [125 I]10 was specific to rodent $\alpha 7$ -nAChRs and that [125 I]10 might be an excellent selective human $\alpha 7$ -nAChR imaging agent.

For the purpose of elucidating the binding mode and efficiency of $\alpha 7$ -nAChR and its high potency ligands, molecular docking was performed. We chose 10 together with previously reported compounds iodo-ASEM to reveal the binding mode and find the differences among the three. The two ligands were successfully docked into the binding pocket (see Fig. S1 in Supplementary Information). Docking results

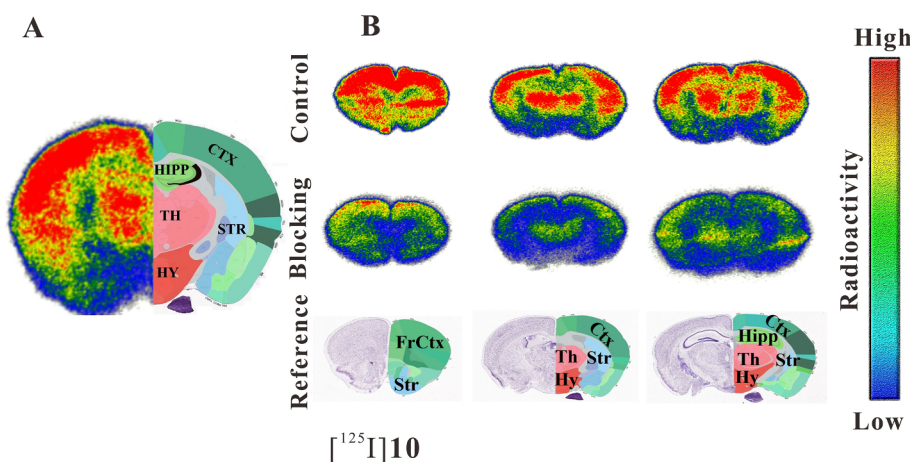


Fig. 7. Ex vivo autoradiography of [^{125}I]10 in Kunming mice. (A) [^{125}I]10 with reference brain sections. (B) Ex vivo autoradiography of [^{125}I]10 in Kunming mice brain sections and control sections (coronal). The presence and distribution of $\alpha 7$ -nAChRs in the sections were confirmed by blocking studies with selective $\alpha 7$ -nAChR ligands.

revealed that the interactions of $\alpha 7$ -nAChR with series ligands were dominated by the substitution of the 1,4-Diazobicyclo[3.2.2]nonane group. The similar docking poses of the ligands indicate that the 3D geometry of the diazobicyclo group may play a vital role in binding affinity. A strong H-bond was observed between Trp145 and the protonated tertiary amine of the nitrogen heterocyclic ring. The protonated tertiary amine laying at the center of the pocket formed three π -H interactions with Trp145, Tyr184 and Tyr191. The predicted binding models demonstrated that the diazobicyclo group was important for the studied ligands and may provide the structural basis for further modifications of $\alpha 7$ -nAChR ligands.

Conclusion

In this paper, we have reported the synthesis, radiobiological evaluations and binding modes of a series of 9H-fluoren-9-one substitutes

derivatives derivatives as potent ligands for $\alpha 7$ -nAChRs. Among the series of compounds, **10** having the best $\alpha 7$ nicotinic receptor binding affinity ($K_i = 2.23 \pm 0.56$ nM), and high selectivity versus $\alpha 4\beta 2$ receptor subtypes, was radiolabeled with ^{125}I .

[^{125}I]10 have good *in vitro* stability, and efficiently entered the Kunming mouse brain, which was then specifically labeled with $\alpha 7$ nicotinic receptors postinjection. Furthermore, blocking studies, *ex vivo* autoradiography and micro-SPECT/CT imaging in mice confirmed the specificity and selectivity of the ligands with $\alpha 7$ -nAChRs. Additionally, docking studies were also performed to rationalize the different potencies of **10** towards $\alpha 7$ -nAChRs and may provide some ideas to design new $\alpha 7$ -nAChR ligands.

Taken together [^{125}I]10 exhibits the excellent properties as a promising SPECT radiotracer for studying $\alpha 7$ -nAChRs both *in vivo* and *in vitro*. Further studies of **10** labeled with ^{123}I and are underway.

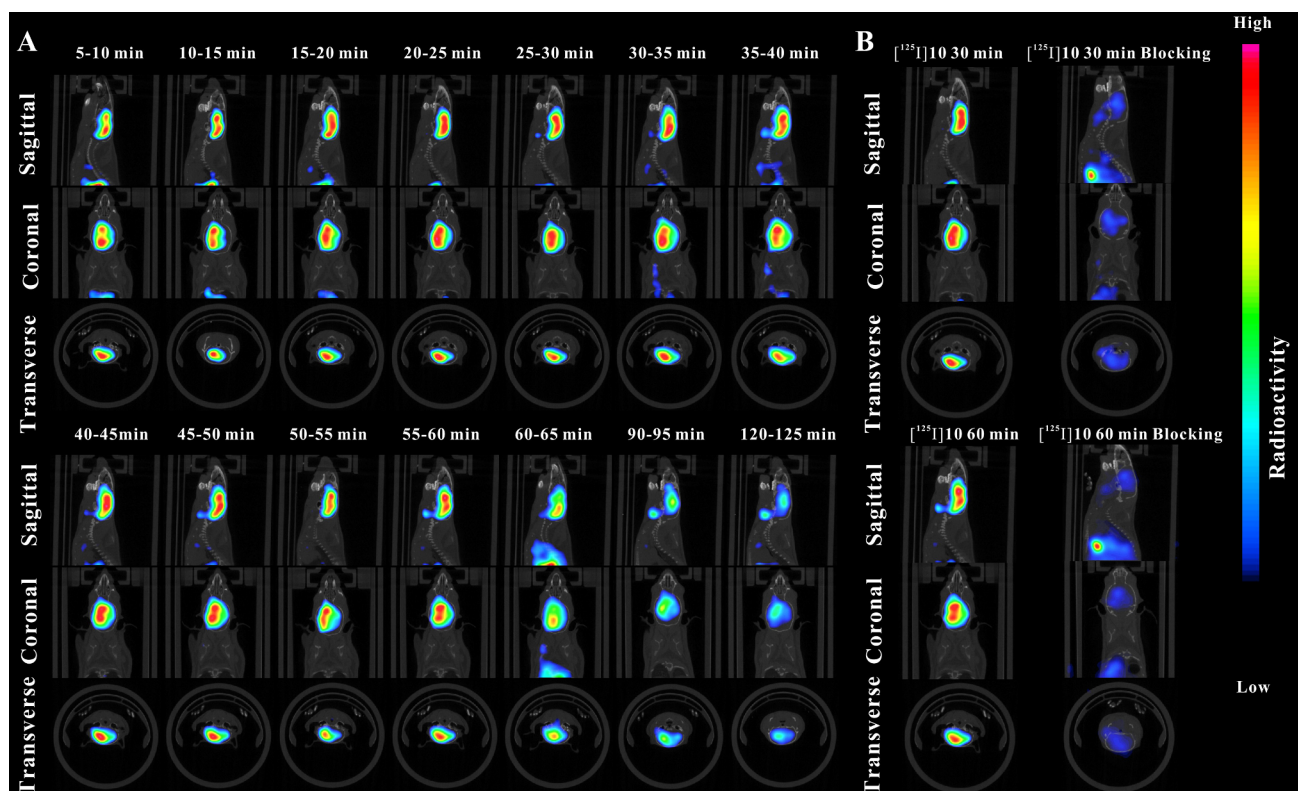


Fig. 8. Dynamic micro-SPECT/CT studies of radio tracers in Kunming mouse (female, 18–22 g). (A) Dynamic micro-SPECT/CT images of [^{125}I]10. (B) Micro-SPECT/CT blocking studies of [^{125}I]10.

Declaration of Competing Interest

The authors declare that they have no known competing financial interests or personal relationships that could have appeared to influence the work reported in this paper.

Acknowledgments

This work was supported by the National Major Scientific and Technological Special Project for “Significant New Drugs Development” (Grant Nos. 2014ZX09507007-001 and 2014ZX09507007-003) and the National Natural Science Foundation of China (Grant No. 21771022). We also thank the Tianjin Institute of Pharmaceutical Research (Tianjin, China) for providing help in the use of Maestro (Shrödinger, LLC, Portland, OR) software package.

Appendix A. Supplementary data

Supplementary data to this article can be found online at <https://doi.org/10.1016/j.bmcl.2019.126724>.

References

1. Gotti C, Zoli M, Clementi F. *Trends Pharmacol Sci.* 2006;27:482.
2. Wu J, Ishikawa M, Zhang J, Hashimoto K. *Int J Alzheimers Dis.* 2010;2010:548913.
3. Dajas-Bailador F, Wonnacott S. *Trends Pharmacol Sci.* 2004;25:317.
4. Gotti C, Clementi F. *Prog Neurobiol.* 2004;74:363.
5. Arias HR. *Brain Res Brain Res Rev.* 1997;25:133.
6. Ishikawa M, Hashimoto K. *Curr Pharm Des.* 2011;17:121.
7. Parri HR, Hernandez CM, Dineley KT. *Biochem Pharmacol.* 2011;82:931.
8. Thomsen MS, Hansen HH, Timmerman DB, Mikkelsen JD. *Curr Pharm Des.* 2010;16:323.
9. Auld DS, Kornecook TJ, Bastianetto S, Quirion R. *Prog Neurobiol.* 2002;68:209.
10. Walling D, Marder SR, Kane J, et al. *Schizophr Bull.* 2016;42:335.
11. Gault LM, Lenz RA, Ritchie CW, et al. *Alzheimers Res Ther.* 2016;8:44.
12. Gault LM, Ritchie CW, Robieson WZ, Pritchett Y, Othman AA, Lenz RA. *Alzheimers Dement (NY).* 2015;1:81.
13. Sedvall G, Farde L, Hall H, et al. *Clin Neurosci.* 1995;3:112.
14. Brust P, Peters D, Deuther-Conrad W. *Curr Drug Targets.* 2012;13:594.
15. Pomper MG, Phillips E, Fan H, et al. *Nucl Med.* 2005;46:326.
16. Gao Y, Mease RC, Olson TT, et al. *Nucl Med Biol.* 2015;42:488.
17. Hashimoto K, Nishiyama S, Ohba H, et al. *PLoS One.* 2008;3:e3231.
18. Deuther-Conrad W, Fischer S, Hiller A, et al. *Eur J Nucl Med Mol Imaging.* 2011;38:1541.
19. Gao Y, Kellar KJ, Yasuda RP, et al. *Med Chem.* 2013;56:7574.
20. Hillmer AT, Li S, Zheng MQ, et al. *Eur J Nucl Med Mol Imaging.* 2017;44:1042.
21. Wang S, Fang Y, Wang H, et al. *Eur J Med Chem.* 2018;159:255.
22. Wong DF, Kuwabara H, Pomper M, et al. *Mol Imaging Biol.* 2014;16:730.